Published in final edited form as:

*Nature*. 2009 August 13; 460(7257): 914–918. doi:10.1038/nature08196.

# Multiple roles for Mre11 at uncapped telomeres

**Yibin Deng**[1,5,@], **Xiaolan Guo**[1,2,5,@], **David O. Ferguson**[3], and **Sandy Chang**[1,4,*]

[1]Department of Genetics, Box 1006, The M.D. Anderson Cancer Center, 1515 Holcombe Blvd., Houston, TX 77030 USA

[2]Institute of Rheumatology and Immunology, North Sichuan Medical College, Nanchong, Sichuan, 637000, P. R. China

[3]Department of Pathology, The University of Michigan Medical School, Ann Arbor, MI 48109, USA.

[4]Department of Hematopathology, The M.D. Anderson Cancer Center, 1515 Holcombe Blvd., Houston, TX 77030 USA

## Abstract

Progressive telomere attrition or uncapping of the shelterin complex elicits a DNA damage response (DDR) as a result of a cell's inability to distinguish dysfunctional telomeric ends from DNA double-strand breaks (DSBs)1. Telomere deprotection activates both ataxia telangiectasia mutated (ATM) and telangiectasia and Rad3-related (ATR) kinase dependent DDR pathways and promotes efficient non-homologous end-joining (NHEJ) of dysfunctional telomeres2–5. The mammalian Mre11-Rad50-NBS1 (MRN) complex interacts with ATM to sense chromosomal DSBs and coordinate global DNA damage responses6, 7. While the MRN complex accumulates at dysfunctional telomeres, it is not known whether mammalian MRN promotes repair at these sites. Here we address this question by utilizing mouse alleles that either inactivate the entire MRN complex or eliminate only the nuclease activities of Mre118. Cells lacking MRN do not activate ATM when telomeric repeat binding factor 2 (TRF2) is removed from telomeres, and Ligase 4 (Lig4) dependent chromosome end-to-end fusions are markedly reduced. Residual chromatid fusions involve only telomeres generated by leading strand synthesis. Strikingly, while cells deficient for Mre11 nuclease activity efficiently activate ATM and recruit 53BP1 to deprotected telomeres, the 3' telomeric overhang persists to prevent NHEJ-mediated chromosomal fusions. Removal of shelterin proteins that protect the 3' overhang in the setting of Mre11 nuclease deficiency restores Lig4 dependent chromosome fusions. Our data suggest a critical role for the MRN complex in sensing dysfunctional telomeres, with Mre11 nuclease activity required to



[*]Correspondence and request for materials should be addressed to S.C.(schang@mdanderson.org).

[5]Present address: Section of Cancer Genetics, The Hormel Institute, University of Minnesota, Austin, MN 55912 USA

[@]These authors contributed equally to this work.

**Author Contributions**

Y.D. designed and guided all experiments, helped write the paper and generated figures. X.G. performed all the experiments presented. D.F. provided Mre11 mouse cell lines for this study and assisted in the interpretation of results. S.C. conceived this study, analyzed and interpreted the data, wrote the paper and finalized the figures.

**Author Information**

The authors declare no competing financial interests.

remove the 3’ telomeric overhang to promote chromosome fusion. Mre11 is also required to protect newly replicated leading strand telomeres from engaging the NHEJ pathway, likely by promoting 5’ strand resection to generate Pot1a-TPP1 bound 3’ overhangs that prevents NHEJ.

The proper maintenance of telomeres is essential for global genome stability. Mammalian telomeres are composed TTAGGG repeats bound to shelterin, a complex of six core proteins, including the double-stranded DNA binding proteins TRF1 and TRF2 and Protection of Telomeres 1 (POT1) that interacts with its binding partner TPP1 to protect single-stranded G-rich overhangs1. Telomeres rendered dysfunctional by the removal of TRF2 are recognized as DSBs, activate ATM and are ligated by the NHEJ pathway to generate fused chromosomes3. The MRN complex recruits ATM to sites of DSBs, where it initiates a signaling cascade leading to checkpoint responses9, 10. While MRN localizes to deprotected telomeres11, 12, its role in NHEJ-mediated repair is not well understood. We sought to uncover the roles of the MRN complex in NHEJ by utilizing two mouse alleles of Mre11: the $Mre11^{\Delta/\Delta}$ null allele that also abolishes the formation of the MRN complex, and the $Mre11^{H129N/\Delta}$ nuclease-deficient allele that eliminates both endo and exonuclease functions of Mre118. To engage the NHEJ pathway, we removed TRF2 from telomeres with retrovirus-mediated shTRF2 in SV40LT immortalized mouse embryonic fibroblasts (MEFs) (Supplemental Fig. 1a). Metaphase spreads harvested 72 to 120h after shTRF2 treatment revealed a progressive increase in the number of fused telomeres until nearly all chromosomes are joined end-to-end (Supplemental Fig. 1b). This telomere fusion phenotype was suppressed when MEFs were first complemented with shRNA-resistant murine TRF2 cDNA prior to shTRF2 treatment (Supplemental Fig. 1c, d, Supplemental table S1), indicating that the telomere fusions observed are not due to off target effects of shTRF2 treatment.

To determine whether Mre11 is required for the DDR initiated by dysfunctional telomeres, mouse embryo fibroblasts (MEFs) containing the conditional $Mre11^{F/\Delta}$ allele were infected with adenovirus expressing Cre recombinase. The floxed Mre11 allele was efficiently deleted, with concomitant loss of Mre11 protein as confirmed by Western blotting (Supplemental Fig. 2b, c). Since TRF2 represses ATM activation at telomeres4, 5, removal of TRF2 from $Mre11^{F/\Delta}$ cells resulted in robust ATM activation, phosphorylation of Chk2 and induction of γ-H2AX and 53BP1 telomere-induced DNA damage foci (TIF) that colocalized with telomeric DNA in 90% of cells examined (Figure 1a, c, Supplemental Fig. 3a). However, both ATM phosphorylation and TIF formation were reduced to 12% in $Mre11^{\Delta/\Delta}$ MEFs in response to TRF2 depletion (Figure 1a, c; Supplemental Fig. 3a). To determine whether the Mre11 nuclease activity is required for ATM activation after induction of telomere dysfunction, $Mre11^{H129N/\Delta}$ MEFs were generated (Supplemental Fig. 2a–c). In contrast to $Mre11^{\Delta/\Delta}$ MEFs, the phosphorylation of ATM and induction of TIFs upon TRF2 depletion in $Mre11^{H129N/\Delta}$ MEFs remained robust (Fig. 1b, d; Supplemental Fig. 3b). These results suggest that ATM phosphorylation in response to TRF2 depletion requires MRN, while the Mre11 nuclease activity is dispensable for this function. At murine telomeres, ATR activation is repressed by Pot1a4, 5. To test whether ATR activation at telomeres requires MRN or Mre11 nuclease activity, shPot1a was utilized to remove Pot1a in $Mre11^{\Delta/\Delta}$ and $Mre11^{H129N/\Delta}$ MEFs. Pot1a depletion resulted in robust ATR

phosphorylation and TIF formation in both cell types (Figure 1e, f, Supplemental Fig. 3c, d), suggesting that Mre11 is not required to activate an ATR-dependent DDR at telomeres due to Pot1a loss.

Our data demonstrate that removal of TRF2 results in telomeres being recognized as DSBs that elicit MRN dependent DDR. To determine whether repair of dysfunctional telomeres is impacted in the setting of Mre11 nuclease deficiency or upon removal of the MRN complex, TRF2 was depleted in $Mre11^{\Delta/+}$, $Mre11^{F/\Delta}$, $Mre11^{\Delta/\Delta}$ and $Mre11^{H129N/\Delta}$ MEFs. While $Mre11^{F/\Delta}$ cells displayed extensive end-to-end chromosome fusions in a Lig4-dependent manner, $Mre11^{\Delta/\Delta}$ cells showed a 15-fold reduction in the number of chromosome-chromosome fusions (Fig 2a, Supplemental Fig, 4a–c and Supplemental Table S2). Unexpectedly, chromosome-chromosome fusions were similarly reduced in nuclease-deficient $Mre11^{H129N/\Delta}$ cells, even though the DDR is activated upon TRF2 loss (Fig 1d, Fig 2a, and Supplemental Table S2). These results suggest a critical role of the Mre11 nuclease activity in mediating NHEJ of dysfunctional telomeres.

The dramatic reduction in the number of chromosome-chromosome fusions observed in $Mre11^{H129N/\Delta}$ cells treated with shTRF2 suggest the possibility that nucleolytic processing of telomeric ends might be required for NHEJ of dysfunctional telomeres. To test this hypothesis, we examined the status of the 3' single-strand overhang using an in gel hybridization assay. In contrast to shTRF2 treated $Mre11^{F/\Delta}$ cells, which showed rapid reduction of the 3' overhang due to NHEJ-mediated processing13, the 3' overhang persists in $Mre11^{\Delta/\Delta}$ and $Mre11^{H129N/\Delta}$ cells with uncapped telomeres (Fig. 2b). Treatment with the 3' end specific exonuclease ExoI revealed that these overhangs are indeed single-stranded telomeric repeats (Supplemental Fig, 5a, b). `The lack of overhang degradation in $Mre11^{H129N/\Delta}$ cells treated with shTRF2 suggests that nucleolytic processing of 3' telomeric overhang by Mre11 may be required for efficient NHEJ of telomeres rendered dysfunctional through the removal of TRF2.

Interestingly, telomere fusions were not completely abolished in shTRF2 treated $Mre11^{\Delta/\Delta}$ cells. Instead, chromosome-orientation FISH (CO-FISH) revealed that ~90% of these rare fusions involved the leading strands of sister chromatids (Fig. 2c, 2d). After telomeric replication, telomeres formed by leading strand synthesis are initially blunt, while lagging strand DNA synthesis result in the formation of 3' overhang after the removal of the last synthesis primer. Leading strand telomeric ends have to be enzymatically processed after replication to produce a 3' overhang that is protective against NHEJ-mediated fusion. We postulate that the MRN complex prevents NHEJ of newly synthesized leading strand telomeres by mediating 5' end resection of the leading strand to generate a 3' overhang. In support of this notion, leading-leading chromatid fusions comprised ~60% of all chromatid fusions in shTRF2 treated $Mre11^{H129N/\Delta}$ cells, suggesting that the nuclease activity of Mre11 is at least in part responsible for the formation of the 3' overhang at the leading strand (Fig. 2c, 2d).

While the Pot1a-TPP1 shelterin sub-complex14 binds to the 3' single-stranded telomeric overhang and represses ATR-mediated DDR4, 5, little is known how the overhang is protected from engaging DNA repair pathway(s). The presence of intact single-stranded

telomeric overhang in shTRF2 treated Mre11$^{\Delta/H129N}$ cells, and the ability of this mutant to activate ATM/ATR signaling pathways represents an unique opportunity to address this question. Using immunostaining and telomere FISH to detect the localization of endogenous TPP1 at single-stranded overhangs and the double stranded telomeric binding protein TRF1 to mark telomeres, we observed a 3.5-fold reduction of TPP1, but not TRF1, at telomeres in Mre11 proficient cells following TRF2 depletion (Supplemental Figs. 6a–c), reinforcing the notion that telomeric accumulation of the Pot1a-TPP1 complex is reduced when TRF2 is depleted15. In contrast, TPP1 immunostaining remained robust in shTRF2 treated Mre11$^{H129N/\Delta}$ cells (Supplemental Figs. 6a–c), suggesting that Pot1a-TPP1 remain complexed to the single-stranded telomeric overhangs in these cells.

We next asked whether removal of Pot1a-TPP1 rendered the overhang amenable to DSB repair. We first depleted TRF2 in Mre11$^{H129N/\Delta}$ MEFs, then removed Pot1a, Pot1b, or TPP1 from the single-stranded overhang using shRNAs (Supplemental Figure 7a). Depletion of Pot1a but not Pot1b resulted in a 3-fold increase in telomere end-to-end fusions (Figure 3a, b), supporting the hypothesis that in mouse cells, Pot1a helps protect telomeres from engaging inappropriate repair, while Pot1b is involved in the protection of the C-strand16–19. Removal of TPP14 from the 3’ overhang of shTRF2 treated Mre11$^{H129N/\Delta}$ cells resulted in a 5-fold increase in chromosome end-to-end fusions, with 30% of all chromosomes fused (Fig. 3a, b, Supplemental Figs. 7a, 8a, b). Taken together, these results suggest that at telomeres lacking TRF2 and Mre11 nuclease activities, the TPP1-Pot1a complex is able to fully protect the telomeric overhang from engaging inappropriate repair pathways.

ATM, ATR and 53BP1 have been implicated in mediating NHEJ of dysfunctional telomeres following removal of TRF25, 20. We found that depletion of ATR, but not ATM, resulted in a 3-fold reduction in the number of end-to-end chromosomal fusions induced by retroviral expression of full-length TPP1$^{\Delta RD}$ in shTRF2 treated Mre11$^{H129N/\Delta}$ cells (Figure 3c, d, Supplemental Figs. 7b, 9a–c). Similarly, depletion of 53BP1 led to a 4-fold reduction of chromosomes fused in Mre11$^{H129N/\Delta}$ MEFs expressing TPP1$^{\Delta RD}$ (Figure 3c, d, Supplemental Fig. 7c). Collectively, these data argue that in the absence of the Pot1a-TPP1 complex, processing of the single-stranded overhang does not require Mre11 nuclease activity to mediate ATR and 53BP1-dependent chromosomal fusions. We postulate that other nucleases in the cell, for example the nucleotide excision repair nuclease ERCC1/XPF that has been shown to remove the 3’ overhang when coupled to the NHEJ machinery13, might substitute for Mre11 nuclease function at this stage.

Finally, we asked which pathway (NHEJ vs. HR) is required for repair of the single-stranded overhang. Removal of Pot1a/TPP1 from Mre11$^{H129N/F}$ MEFs resulted in elevated HR at telomeres, detected as a 5-fold increase in telomere sister chromatid exchanges (T-SCEs)21 (Supplemental Fig. 10a, b). Interestingly, T-SCEs were not increased significantly in Pot1a/TPP1 depleted Mre11$^{H129N/\Delta}$ cells, suggesting that the Mre11 nuclease activity plays an important role in telomeric HR (Supplemental Fig. 10a–c). When TRF2 is removed from Pot1a/TPP1 depleted Mre11$^{H129N/\Delta}$ cells, robust Lig4 dependent chromosomal fusions were observed (Fig. 4a–c). However, T-SCE levels in these cells remained similar to those observed in control cells (Fig. 4d, Supplemental Fig. 11). These results supports the

hypothesis that the main function of Pot1a-TPP1 is to repress HR at telomeres, while TRF2 is primarily responsible to repress NHEJ at telomeres.

The data presented here demonstrate multiple roles for the MRN complex at telomeres. Mre11 interacts with TRF2 and localizes to telomeres throughout the cell cycle11. Together with TRF2, it plays a protective role in preventing NHEJ-mediated fusion of leading strand telomeric DNA after replication, likely by promoting 5' leading strand resection to generate Pot1a-TPP1 bound 3' overhangs that prevents NHEJ (Supplemental Fig. 12). While the Mre11 nuclease activity plays a role in this process, additional factors are likely to be involved22. One such candidate is CtIP23, 24, since recent data suggests that the yeast homolog Sae2 cooperates with Mre11 to remove nucleotides at DSBs in a 5'-3' endonucleolytic manner before extensive resection is performed by other nucleases including ExoI and Dna225–26. However, generation of 3' single-stranded overhangs has the undesired consequence of initiating inappropriate HR at telomeres. Indeed, the Mre11 nuclease activity is required for telomere HR after Pot1a-TPP1 is removed from the 3' overhang. Since initiation of HR requires RPA binding to single-stranded DNA, we speculate that the Pot1a-TPP1 complex represses HR by preventing RPA access to the 3' overhang.

Removal of TRF2 from telomeres stimulates the MRN complex to activate ATM and 53BP1 to promote NHEJ. Surprisingly, removal of TRF2 also liberates the Mre11 3'-5' nuclease activity to processes 3' telomeric overhangs prior to NHEJ of chromosome ends. Since single stranded telomeric overhangs are incompatible with DNA ligation3, we speculate that degradation of the 3' overhang by Mre1127, likely in conjunction with other components of the NHEJ pathway13, is required to generate telomeric substrates amenable for joining by Lig4. This model is supported by the observation that Mre11 nuclease activities are required for efficient NHEJ during class switch recombination in developing lymphocytes28.

Our studies also uncover an unexpected role for the Pot1a-TPP1 complex in protecting the 3' overhang from NHEJ in the absence of TRF2 and Mre11 nuclease activity. Since TRF2 is thought to be essential for the formation of the t-loop structure proposed to protect chromosome ends from engaging the NHEJ pathway, our result support the notion that under certain conditions the t-loop is dispensable for telomere end protection29. We suggest that the Pot1a-TPP1 complex cooperates with TRF2-Rap1 during telomere replication, when the t-loop is transiently lost, to protect the integrity of linear chromosomal ends30.

## Methods Summary

### Generation of MEFs and conditional deletion of Mre11

MEFs were isolated from E13.5 embryos obtained from crosses between $Mre11^{F/\Delta}$ and $Mre11^{F/H129N}$ mice and grown in standard culture conditions. PCR based genotyping was performed as described8. Primary MEFs were immortalized at passage 2 by transfection with pBabeSV40LT. To delete Mre11, MEFs with different genotypes were treated by adeno-Cre at multiplicities of infection (MOIs) of 500. Depletion of Mre11 was confirmed by PCR and Western Blot.

### shRNA interference

Two shRNA-TRF2s were generated in pSuper as described31. To generate Retro-pSuper constructs, *Eco*R1- and *Xho*I-digested insert from pSuper was subcloned into the same site into Retro-pSuper vector. The shRNA target sequences for mouse TRF2 is: shRNA–TRF2-1: 5'-CTGTCATTATTTGTATC AA-3'; shRNA-TRF2-2: 5'-GAACAGCTGTGATGAT-TAA-3'. The target sequence of shRNA-TRF2-2 was changed to 5'-CGT ACT GCA GTC ATG ATC -3' by standard site-directed mutagenesis to create shRNA-TRF2-2 resistant construct Retro-pSuper shTRF2-2-M (Stratagene). Lentivirus based shRNAs for Ligase IV, Mre11 and 53BP1 were purchased from Sigma (sequences available upon request). Published target sequences5 were constructed into Retro-pSuper and used for knockdown of ATR. shRNAs for Pot1a, Pot1b, TPP1 and TPP1$^{\Delta RD}$ were as described4. Retrovirus or lentivirus-mediated efficient knockdown of target genes was verified by either RT-PCR or immunoblotting.

## Methods

### Mouse Genotyping

Mre11 genotyping was performed as described8. The following primers are used: Forward 5 '-TACAAAAGGTTGAAAATTTGAGAAGC-3 ', Reverse 5 '- TGTAATTGCAGGT-CCTTAAAGGC-3'. The thermocycling conditions are 36 cycles of 95°C for 30 sec, 52°C for 1 min, and 72°C for 1 min.

### RNA isolation, RT-PCR

RNA was isolated from approximately $10^6$ cells with the Qiagen RNAeasy kit. RT-PCR was performed with the oligo-dT RT-PCR system according to the protocol provided by the manufacturer (Invitrogen). The following primers for mPot1a: Forward 5'-GATGAC-GTCACAGGCGCCTAGG-3'; Reverse 5'-TCCCATACACACTGCACTCAATGG-3'. mPot1b: Forward 5'-CTTTAAGCCTCCGGCCTTAAGCAAAGG-3'; Reverse: 5'-CTT-GGACATGATTATCAGCAACGACAATGTCTAC-3'. mTPP1: Forward 5'-ATGTCC-GATTCAGGGTTGCTGG-3'; Reverse 5'-TCATACCTGGGTTAACTCAGACTCT-GACTC-3'. mGAPDH: Forward 5'-TCACCACCATGGAGAAGGC-3'; Reverse 5'-GC-TAAGCAGTTGGTGGTGCA-3'.

### Immunoblotting

Cell extracts were isolated and Western Blot was performed as described4. Antibodies are: phospho-ATM Ser 1981(#20772) from Rockland; phospho-ATR (#2853S), ATR (#2790S) and Mre11 (#4895) are from Cell Signaling; Chk2 (#611570) is from BD Biosciences; γ-tubulin and HA are from Sigma; γH2AX (#05–636) is from Upstate; anti-53BP1 antibody obtained from Dr. Carpenter at UT Medical School; anti-TRF1 and TRF2 antibodies obtained from Dr. Karlseder at Salk Institute.

### IF (Immunofluorescence) and TIF (Telomere dysfunction Induced Foci) analysis

IF and TIF assay for cells with different genotypes grown on coverslips were performed as described previously4 using the primary antibody TRF1, TPP1, 53BP1 or γ-H2AX.

Secondary antibodies against mouse or rabbit were labeled with Alexa 488 (Molecular Probes) and Rhodamine Red-X (RRX, Jackson) respectively. For TIF assay the same primary and secondary antibodies as above using a Tamra-$(TTAGGG)_3$ PNA telomere probe (Applied Biosystems). DNA was counterstained with 4.6-diamidino-2-phenylindole (DAPI) and slides were mounted in 90% glycerol/10% PBS containing 1 μg/mL p-phenylene diamine (Sigma). Digital images were acquired and analyzed as described4. Only cells with 5 ≥ 53BP1 or γ-H2AX signals co-localized with telomere signal (TTAGGG)n were scored.

### Telomere fluorescence *in situ* hybridization (FISH) and CO-FISH

Cells were harvested at indicated time points and fixed, FISH and CO-FISH were performed as described previously4, 17. Hybridization of metaphase spreads was performed with TRITC-OO-$(TTAGGG)_4$ peptide nucleic-acid probes (Applied Biosystems). For CO-FISH, metaphase spreads were incubated sequentially with 5'-Tam-OO-$(CCCTAA)_4$-3' and 5'-FITC-OO-$(TTAGGG)_4$-3' probes. Control experiments were performed to ensure that the CO-FISH signals were dependent on the incorporation of BrdU and that the procedure did not generate signals due to unintended denaturation of the telomeric DNA. A minimum of 500 chromosome ends were scored blindly for each genotype, and pairwise comparisons for statistical significance were made by Student's t test. Differences between genetic backgrounds were considered significant only when p values were less than 0.01. Digital Images were captured and processed with MetaMorph Premier (Molecular Devices).

### In-gel Telomeric G-overhang assay

In-gel G-overhang assay was performed essentially as described17. Following pulse-field gel electrophoresis, gels were dried down at 40°C and prehybridized at 50°C for 1 h in Church mix (0.5 M $Na_2HPO_4$ (pH 7.2), 1 mM EDTA, 7% SDS, and 1% BSA), followed by hybridization at 50°C overnight with an end-labeled $(CCCTAA)_4$ oligonucleotide. After hybridization, gels were washed three times with 4 × SSC for 30 min and once with 4 × SSC/0.1% SDS. Gels were exposed to PhosphoImager screens. Following G-overhang assay, gels were alkali denatured (0.5 M NaOH and 1.5 M NaCl), neutralized (3 M NaCl and 0.5 M Tris–HCl, pH 7.0), rinsed with $H_2O$, and reprobed with the $(CCCTAA)_4$ oligonucleotide at 55°C and then processed as previously. To determine the relative overhang signal, the signal intensity for each lane was determined before and after denaturation using Imagequant software. The G-overhang signal was normalized to the total telomeric DNA and this normalized value was compared between samples.

## Supplementary Material

Refer to Web version on PubMed Central for supplementary material.

## Acknowledgements

We are grateful to Mingcai Zhao, Zhan Lu and Puneeth Iyengar for technical help. Both Jan Karlseder and Philip Carpenter are thanked for providing antibodies. S. C acknowledges generous financial support from the NIA (RO1 AG028888), the NCI (RO1 CA129037), the Welch Foundation, the Susan G. Koman Race for the Cure Foundation, the Abraham and Phyllis Katz Foundation and the Michael Kadoorie Cancer Genetic Research Program. Y.D. was supported by an NCI Howard Temin Award (K01CA124461).

## References


1. Palm W, de Lange T. How shelterin protects mammalian telomeres. Annu. Rev. Genet. 2008; 42:301–334. [PubMed: 18680434]
2. van Steensel B, Smogorzewska A, de Lange T. TRF2 protects human telomeres from end-to-end fusions. Cell. 1998; 92:401–413. [PubMed: 9476899]
3. Celli GB, de Lange T. DNA processing is not required for ATM-mediated telomere damage response after TRF2 deletion. Nature Cell Biol. 2005; 7:712–718. [PubMed: 15968270]
4. Guo X, et al. Dysfunctional telomeres activate an ATM-ATR-dependent DNA damage response to suppress tumorigenesis. EMBO J. 2007; 26:4709–4719. [PubMed: 17948054]
5. Denchi EL, de Lange T. Protection of telomeres through independent control of ATM and ATR by TRF2 and POT1. Nature. 2007; 448:1068–1071. [PubMed: 17687332]
6. D'Amours D, Jackson SP. The Mre11 complex: at the crossroads of DNA repair and checkpoint signalling. Nature Rev. Mol. Cell. Biol. 2002; 3:317–327. [PubMed: 11988766]
7. Lee JH, Paull TT. ATM activation by DNA double-strand breaks through the Mre11-Rad50-Nbs1 complex. Science. 2005; 308:551–554. [PubMed: 15790808]
8. Buis J, et al. Mre11 nuclease activity has essential roles in DNA repair and genomic stability distinct from ATM activation. Cell. 2008; 135:85–96. [PubMed: 18854157]
9. Falck J, Coates J, Jackson SP. Conserved modes of recruitment of ATM, ATR and DNA-PKcs to sites of DNA damage. Nature. 2005; 434:605–611. [PubMed: 15758953]
10. Deng Y, Chan SS, Chang S. Telomere dysfunction and tumour suppression: the senescence connection. Nature Rev. Cancer. 2008; 8:450–458. [PubMed: 18500246]
11. Zhu XD, Kuster B, Mann M, Petrini JH, de Lange T. Cell-cycle-regulated association of RAD50/MRE11/NBS1 with TRF2 and human telomeres. Nature Genet. 2000; 25:347–352. [PubMed: 10888888]
12. Takai H, Smogorzewska A, de Lange T. DNA damage foci at dysfunctional telomeres. Curr. Biol. 2003; 13:1549–1556. [PubMed: 12956959]
13. Zhu XD, et al. ERCC1/XPF removes the 3' overhang from uncapped telomeres and represses formation of telomeric DNA-containing double minute chromosomes. Mol. Cell. 2003; 12:1489–1498. [PubMed: 14690602]
14. O'Connor MS, Safari A, Xin H, Liu D, Songyang Z. A critical role for TPP1 and TIN2 interaction in high-order telomeric complex assembly. Proc. Natl Acad. Sci. USA. 2006; 103:11874–11879. [PubMed: 16880378]
15. Hockemeyer D, et al. Telomere protection by mammalian Pot1 requires interaction with Tpp1. Nature Struct. Mol. Biol. 2007; 14:754–761. [PubMed: 17632522]
16. Hockemeyer D, Daniels JP, Takai H, de Lange T. Recent expansion of the telomeric complex in rodents: Two distinct POT1 proteins protect mouse telomeres. Cell. 2006; 126:63–77. [PubMed: 16839877]
17. Wu L, et al. Pot1 deficiency initiates DNA damage checkpoint activation and aberrant homologous recombination at telomeres. Cell. 2006; 126:49–62. [PubMed: 16839876]
18. Hockemeyer D, Palm W, Wang RC, Couto SS, de Lange T. Engineered telomere degradation models dyskeratosis congenita. Genes Dev. 2008; 22:1773–1785. [PubMed: 18550783]
19. He H, et al. Pot1β deletion and telomerase haploinsufficiency in mice initiate an ATR-dependent DNA damage response and elicit phenotypes resembling dyskeratosis congenita. Mol. Cell. Biol. 2009; 29:229–240. [PubMed: 18936156]
20. Dimitrova N, Chen YC, Spector DL, de Lange T. 53BP1 promotes non-homologous end joining of telomeres by increasing chromatin mobility. Nature. 2008; 456:524–528. [PubMed: 18931659]
21. Bailey SM, Cornforth MN, Kurimasa A, Chen DJ, Goodwin EH. Strand-specific postreplicative processing of mammalian telomeres. Science. 2001; 293:2462–2465. [PubMed: 11577237]
22. Hopkins BB, Paull TT. The *P. furiosus* MRE11/RAD50 complex promotes 5' strand resection at a DNA double-strand break. Cell. 2008; 135:250–260. [PubMed: 18957200]

23. Limbo O, Chahwan C, Yamada Y, de Bruin RA, Wittenberg C, Russell P. Ctp1 is a cell-cycle-regulated protein that functions with Mre11 complex to control double-strand break repair by homologous recombination. Mol. Cell. 2007; 28:134–146. [PubMed: 17936710]
24. Sartori AA, Lukas C, Coates J, Mistrik M, Fu S, Bartek J, Baer R, Lukas J. Human CtIP promotes DNA end resection. Nature. 2007; 450:509–514. [PubMed: 17965729]
25. Mimitou EP, Symington LS. Sae2, Exo1 and Sgs1 collaborate in DNA double-strand break processing. Nature. 2009; 455:770–774. [PubMed: 18806779]
26. Zhu Z, Chung WH, Shim EY, Lee SE, Ira G. Sgs1 helicase and two nucleases Dna2 and Exo1 resect DNA double-strand break ends. Cell. 2008; 134:981–994. [PubMed: 18805091]
27. Paull TT, Gellert M. The 3' to 5' exonuclease activity of Mre11 facilitates repair of DNA double-strand breaks. Mol. Cell. 1998; 1:969–979. [PubMed: 9651580]
28. Dinkelmann M, Spehalski E, Stonehamx StonehamT, Buis J, Wu Y, Sekiguchi JM, Ferguson DO. Multiple functions of MRN in end-joining pathways during isotype class switching. Nature Struct. Mol. Biol. 2009 (in press).
29. Wang X, Baumann P. Chromosome fusions following telomere loss are mediated by single-strand annealing. Mol. Cell. 2008; 31:463–473. [PubMed: 18722173]
30. Verdun RE, Karlseder J. The DNA damage machinery and homologous recombination pathway act consecutively to protect human telomeres. Cell. 2006; 127:709–720. [PubMed: 17110331]
31. Deng Y, Ren X, Yang L, Lin Y, Wu X. A JNK-dependent pathway is required for TNFα-induced apoptosis. Cell. 2003; 115:61–70. [PubMed: 14532003]

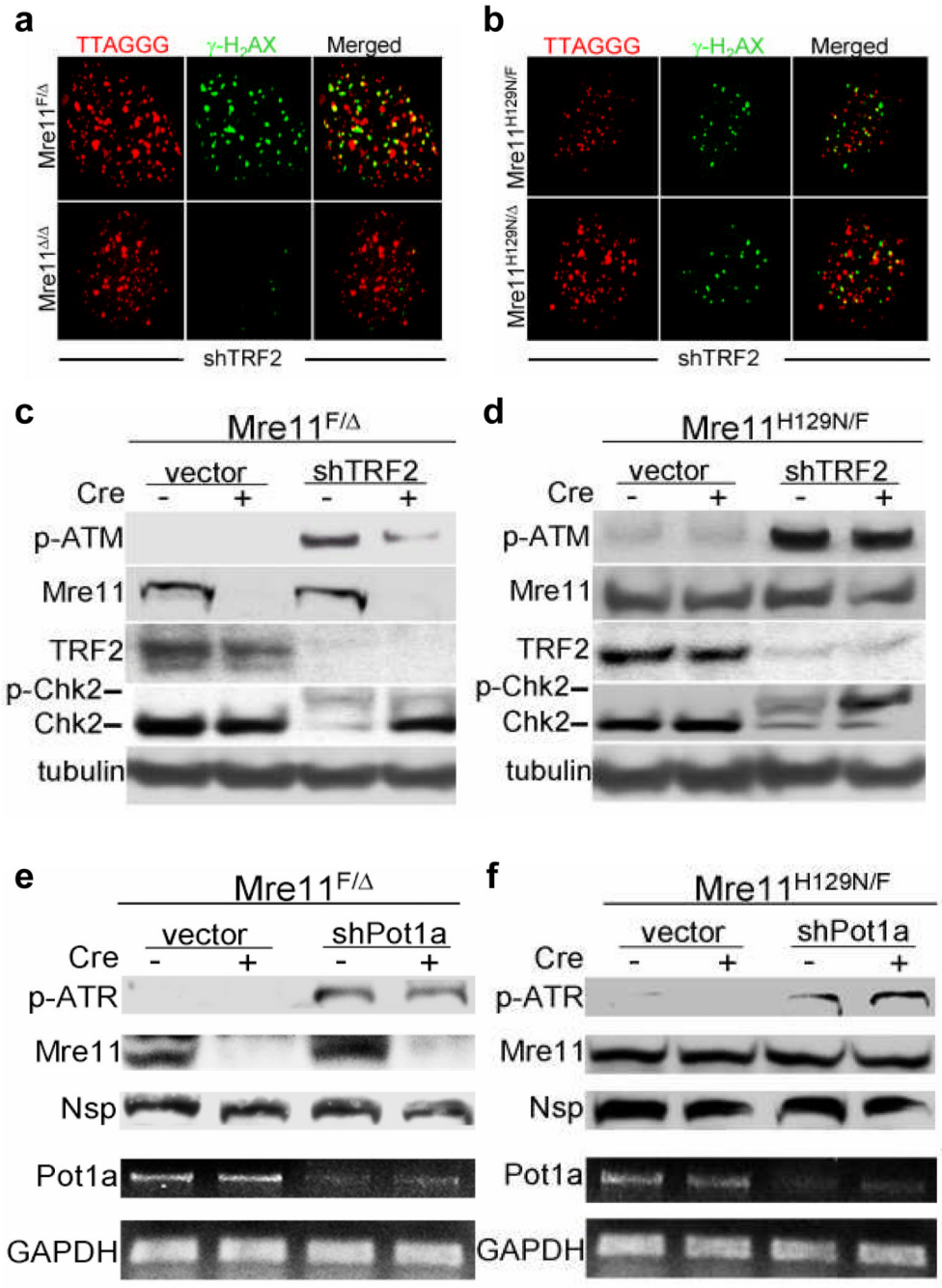


**Figure 1. Activation of ATM, not ATR, following TRF2 depletion requires the MRN complex but not Mre11 nuclease activity**

**a, b**, γ-H2AX-positive TIFs in MEFs of the indicated genotypes after TRF2 depletion in Mre11 deficient SV40LT immortalized MEFs (**a**) and Mre11 nuclease activity deficient MEFs (**b**). **c, d**, Western blots detecting TRF2, Mre11, ATM and Chk2 phosphorylation after shTRF2 treatment in Mre11 deficient SV40LT immortalized MEFs (**c**) and Mre11 nuclease activity deficient MEFs (**d**). Tubulin served as loading control. **e, f**, Immunoblots for Mre11 and ATR phosphorylation and RT-PCR to detect Pot1a and GAPDH transcripts

after shPot1a infection of Mre11 deficient SV40LT immortalized MEFs (**e**) and Mre11 nuclease activity deficient MEFs (**f**). Nsp: non-specific protein served as loading control.

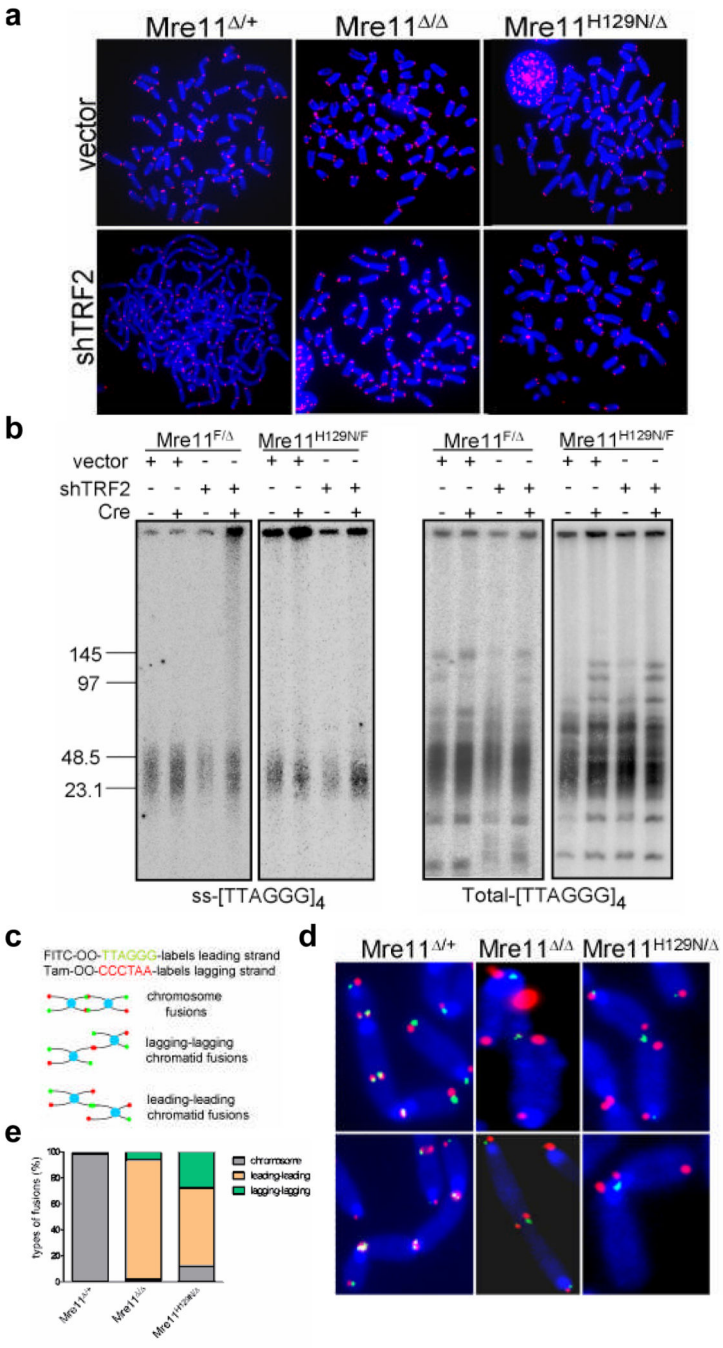


**Figure 2. The MRN complex and Mre11 nuclease activity are required for NHEJ of telomeres lacking TRF2**

**a**, MEFs of the indicated genotypes were treated with control vector or shTRF2 for 120h, metaphases were prepared and telomere fusions were visualized by telomere PNA-FISH (red) and DAPI (blue). **b**, In-gel hybridization assay using a CHEF gel to fractionate genomic DNA, then hybridized *in situ* to a $(CCCTAA)_4$ probe to detect the 3' overhang under native conditions (left) and under denatured condition (right) to detect total TTAGGG repeats (right). **c**, (Left panel): Telomeric probes used in CO-FISH experiments [FITC-OO-

$(TTAGGG)_4$; green, labels the leading strand and Tam-OO-$(CCCTAA)_4$; red, labels the lagging strand] and schematic of fusion products expected in chromosome-chromosome, leading-leading chromatid and lagging-lagging chromatid fusions. (Right panel): Fusion products of shTRF2 treated cells of the indicated genotypes analyzed by CO-FISH. DNA was detected by DAPI (blue). Representative images are shown. **d**, Quantification of the types of fusions observed in cells of the indicated genotypes as a percentage of total fusions observed following TRF2 depletion. A minimum of 150 independent fusion events with telomeric signals at the sites of fusions were characterized per genotype.

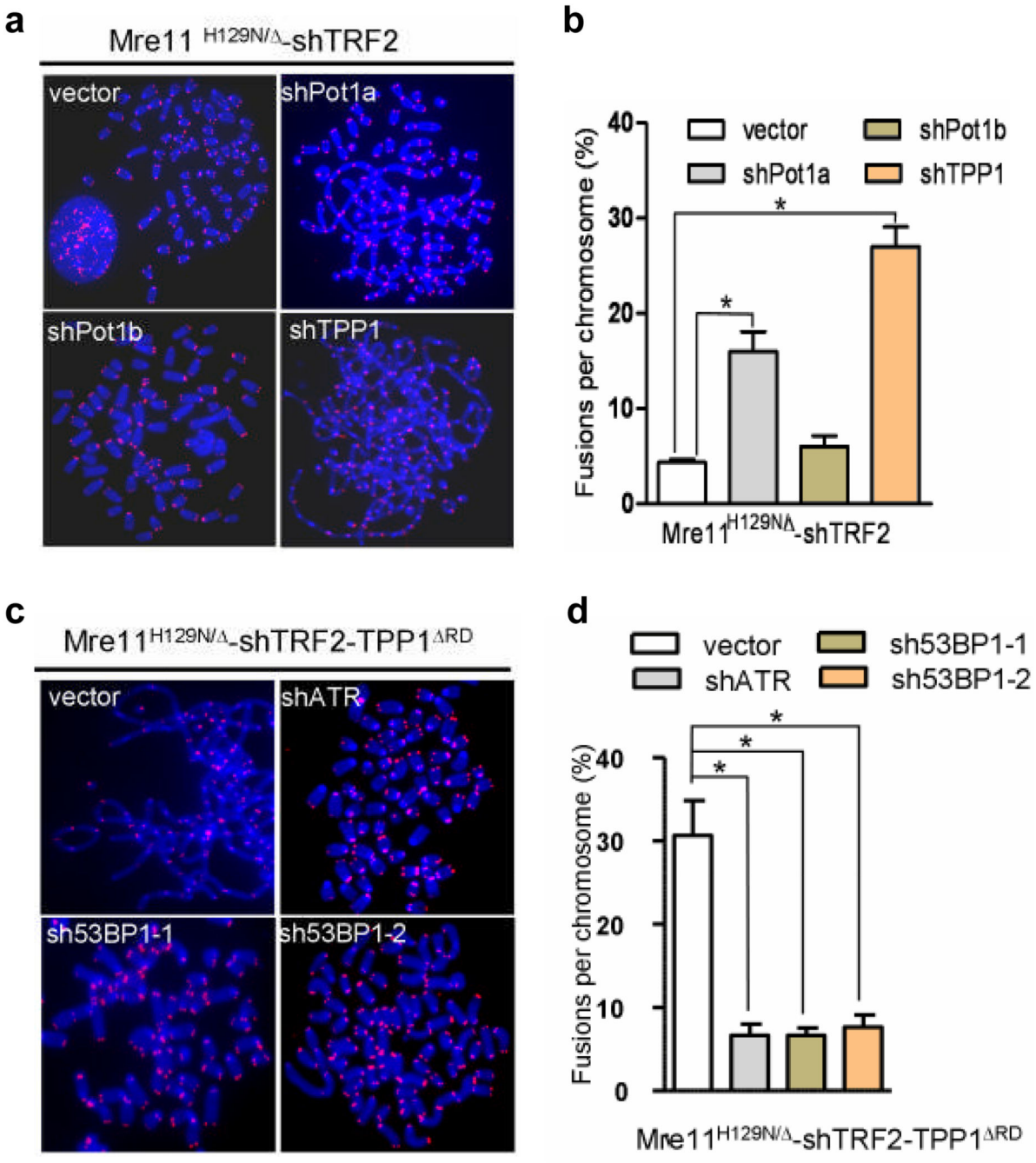


**Figure 3. Pot1a-TPP1 complex protects single-stranded overhangs from engaging in inappropriate repair**

**a**, Depletion of Pot1a or TPP1, but not Pot1b, results in pronounced telomere fusions in metaphase spreads from shTRF2 treated Mre11$^{H129N/\Delta}$ MEFs, with telomeric PNA-FISH (red) and DAPI (blue). **b**, Quantitation of telomere fusions from representative images are shown in (**b**). Error bars, s.d.; n ≥ 350, asterisk, p<0.001. **c**, Depletion of ATR or 53BP1 inhibits chromosomal fusions generated by expression of TPP1$^{\Delta RD}$ cDNA and removal of

TRF2 in Mre11$^{H129N/\Delta}$ MEFs. **d**, Qunatification of telomere fusions from representative images shown in **(c)**. Error bars, s.d.; n ≥ 900, asterisk, p<0.001.

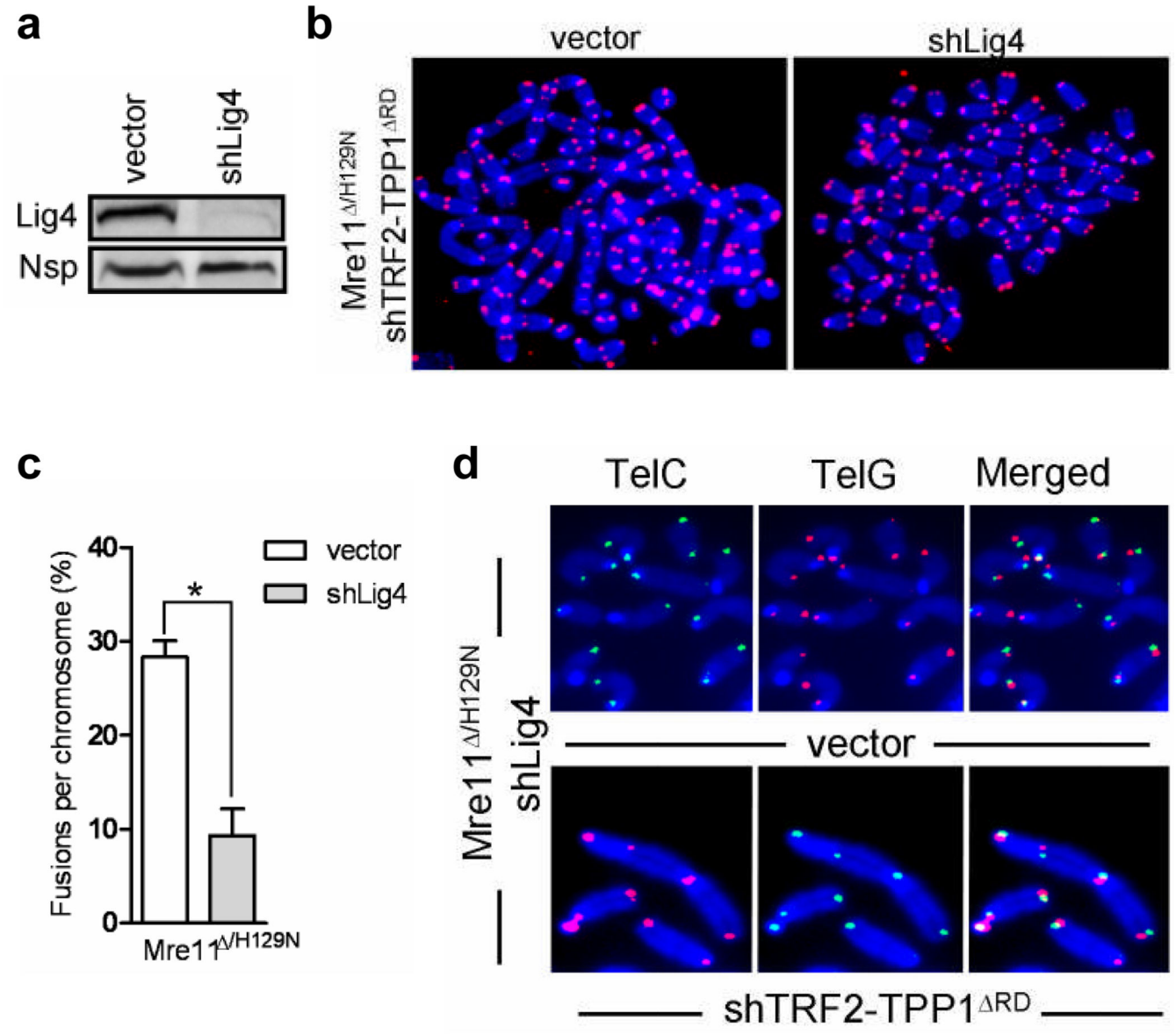


**Figure 4. Ligase IV is required for NHEJ of single-stranded telomeric overhangs**

**a**, Immunoblot demonstrating that shLig4 efficiently depletes Lig4 from Mre11$^{H129N/\Delta}$ nuclease-deficient MEFs expressing TPP1$^{\Delta RD}$ and shTRF2. Nsp: nonspecific protein used as loading control. **b**, Lig4 is required for chromosomal fusions in Mre11$^{H129N/\Delta}$ nuclease-deficient MEFs expressing TPP1$^{\Delta RD}$ and shTRF2. **c**, Quantitation of number of fusions per chromosome from representative images shown in (b). Error bars, s.d.; n ≥ 850, asterisk, $p<0.001$. **d**, T-SCEs in Mre11$^{H129N/\Delta}$ nuclease-deficient MEFs deficient in Lig4, TRF2 and TPP1. CO-FISH was performed using FITC-OO-TTAGGG$_4$ (green) and Tam-OO-(CCCTAA)$_4$ (red) probes.